УДК 539.2:669.24 https://doi.org/10.15407/materials2025.10-11.050

Laser-enhanced electrodeposition of local zinc coatings

V. V. Tytarenko*, V. N. Gorev, A. N. Turinov, T. E. Voronko

Dnipro University of Technology
49005, Dnipro, Ukraine, av. Dmytra Yavornytskoho, 19
*E-mail: tytarenko.valentina@gmail.com

The study presents the developed method of obtaining local zinc coatings without masks using a pulsed laser, the beam of which is focused on a cathode located in a galvanic bath. We observe an acceleration of the process of electrodeposition of zinc films by 9.4 times at a laser power density of $70 \cdot 10^7$ W/m^2. Scanning of the cathode surface by laser radiation leads to the localised formation of a metallic coating whose configuration corresponds to the trajectory of the laser beam.

***Keywords**: electrodeposition, laser radiation, cathode overpotential, area of thermal influence, local electrolytic coating.*

Introduction

Recently, the electrodeposition process stimulated by laser irradiation to accelerate the electrometallisation process has been the subject of increased interest of the metal coatings industry [1—5]. In the manufacturing process of microelectronic devices, existing processes for creating complex metallised structures require several particularly complex steps for mask fabrication, photolithography process, etc. This increases the complexity of process control and production cost. The development of laser-enhanced metal coating process is a very promising technology for fast maskless selective film deposition.

The application of local electrolytic zinc coatings is promising for microelectronics in order to protect critical components from corrosion and to apply microdoses of zinc-containing solder for small-sized parts.

The purpose of this work was to determine the optimal conditions of local laser-enhanced electrodeposition of zinc in the form of spots and lines for the formation of contact pads or images of integrated circuit topology.

Materials and methods

Electrodeposition of zinc films was carried out from a standard sulfuric acid electrolyte of the following composition (g/l): $ZnSO_4 \cdot 7H_2O$ — 250, Na_2SO_4 — 75, $Al(SO_4)_3$ — 30, pH — 4. The experimental facility (Fig. 1) was assembled on the basis of a solid-state ruby laser KVANT-12. Generation on ruby was carried out in pulse-periodic mode at the wavelength of laser radiation λ equal to 694 nm, at the generation frequency f — 10 Hz with the energy of radiation in

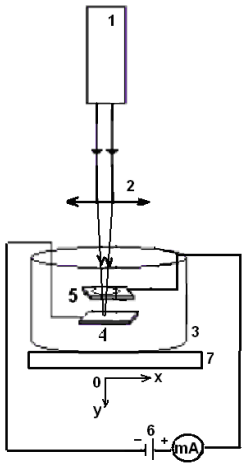

Fig. 1. Schematic diagram of the experimental facility: 1 — radiation source (solid-state ruby laser KVANT-12: λ = 694 nm, ω = = (70—95)·10^7 W/m^2); 2 — focusing lens; 3 — electrolytic cell; 4 — cathode; 5 — anode; 6 — constant current source; 7 — coordinate table.

a pulse W — 2,2—3,0 J, pulse duration t_p — 2—5 ms, radius of focused laser beam r_0 — 0,5 mm. At the energy of radiation 2,2 J the intensity of laser radiation ω was 70·10^7 W/m^2. The working table served for fixing and positioning of the cathode surface relative to the fixed focussed laser beam. The scanning speed υ of the laser beam during the deposition of zinc tracks was 3 mm/s.

Copper substrate was used as a cathode during process of electroplating. The substrate was pre-processed in the following way. At first it was polished mechanically by polishing paste based on chromium oxide and a diamond paste. 5% nitric acid solution was used for chemical polishing. Chemical polishing reduced roughness and removed strain hardening resulted from mechanical polishing. After that substrates were degreased in Vienna lime to remove etching sludge and washed with distilled water. Anode was represented by a of pure zinc plate that allowed maintaining invariable concentration of zinc ions that gave a positive effect on repeatability of tests.

The temperature of the aqueous electrolyte solution was determined using a copper-constantan thermocouple. The steady-state value of thermo–emf was established for a time of 150—200 s and measured with a digital voltmeter.

The polarization dependences were recorded in the potentiodynamic mode on a P-5827M potentiostat at a potential sweep rate of 10 mV/s. The measurements were carried out in a three-electrode electrolytic cell. A copper plate was used as the working electrode (cathode). The reference electrode was a silver chloride electrode, and the auxiliary electrode was a platinum electrode.

Transmittance spectrum of electrolyte water solutions in the ultraviolet and visible range were recorded by spectrophotometer NIR 61.

Metallographic studies of structure were fulfilled using microscope ”Neophot-21”.

Results and discussion

According to the results of the study of transmittance spectra of a number of aqueous solutions of electrolytes (Fig. 2) the zinc electrolyte has a relatively high transmittance (55,8%) at the length of the used laser radiation (λ = 694 nm).

The analysis of cathodic polarisation curves (Fig. 3) showed that with increasing cathodic potential the curve of zinc reduction at switched off source of laser radiation (curve 2) is located below the curve of laser-enhanced

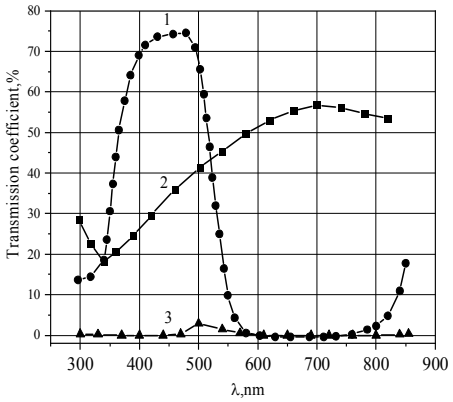

Fig. 2. Transmittance spectral curves of aqueous electrolyte solutions: 1 — copper-plating electrolyte; 2 — zinc-plating electrolyte; 3 — nickel-plating electrolyte.

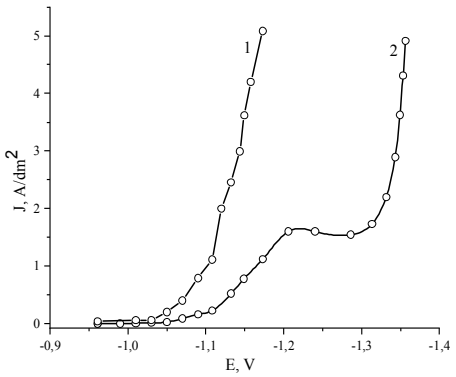

Fig. 3. Potentiodynamic volt-ampere dependence obtained in the zinc plating electrolyte: 1 — laser-enhanced electrodeposition mode; 2 — direct current electrodeposition mode.

electrodeposition process (curve 1). In the laser-enhanced electrodeposition mode, an increase in the current density and a shift of the cathode potential towards positive values are observed in comparison with the deposition mode using direct current without laser irradiation.

The efficiency of laser influence can be estimated by means of the laser acceleration coefficient $K = \frac{J}{J_0}$, which is also a measure of the selectivity of the process and is equal to the ratio of the current density of the laser-enhancedelectrodeposition mode (J) to the current density when the laser radiation source is switched off (J_0). From the cathodic polarisation curves (Fig. 3) we can see that the highest value of K = 9,4 falls on the value of the cathode potential E = −0,97 V for the laser power density of $70 \cdot 10^7$ W/m^2.

Studies have shown that at potential E > −0,97 V zinc electrodeposition at switched off source of laser radiation is not visually observed. At E < −0,99 V, which corresponds to the cathode current density at laser irradiation of 0,8 A/dm^2, uniform coverage of the entire surface of the copper cathode with a layer of metallic zinc is observed.

Analysis of electrodeposited zinc surface morphology showed that use of external laser exposure of cathode area in the process of electrodeposition resulted in transformation of surface morphology in comparison with coatings produced by direct current (DC) application without laser exposure.

Process of cathodic zinc reduction from sulphate electrolyte is accompanied by release of hydrogen which passivates cathode surface due to adsorption across its whole surface. Analysis of electroplated coatings (Fig. 4, *a*), showed formation of surface blisters which look like “frozen” gas bubbles and represent such superficial defects.

In laser-enhanced electrodeposition mode zinc coating internal stress in the radiation field decreases, coating has a developed surface (Fig. 4, *b*).

According to the experimental data the process of local laser-enhanced electrodeposition of zinc on the copper base is most expediently carried out at E = −0,97 V and J = 4,6 A/m^2.

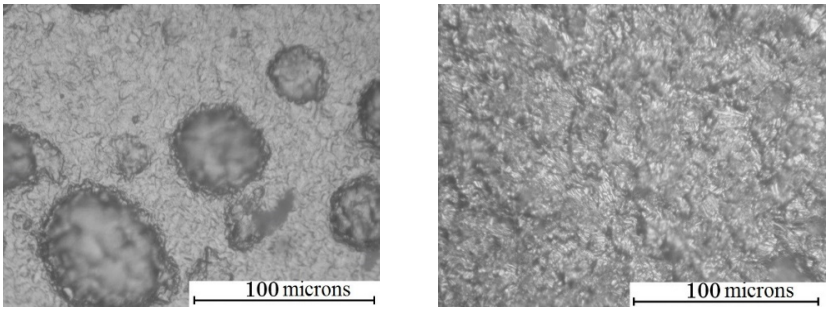

a *b*

Fig. 4. Morphology of laser-enhanced electroplated zinc surface: *a* — in radiation zone; *b* — out of radiation zone.

The increase in the deposition current density under laser irradiation is associated with local heating of the solution-electrode interface and a concomitant increase in mass transfer, which is caused by mixing of the solution near the cathode surface [6—9]. Laser acceleration of the zinc deposition process is due to the thermal effect, which was established by probing the laser irradiation zone using a copper-constantan thermocouple, which showed heating of the central region of the focused laser beam with radius r_0 = 0,5 mm from 296 to 332 K.

Current density and laser acceleration coefficient of the electrodeposition process are functions of the electrolyte solution temperature (Arrhenius-type dependences):

$$j \approx \exp[W / R(T_0 + \Delta T)], \quad (1)$$

$$K_y \approx \exp[W\Delta T / (R(T_0 + \Delta T)T_0)], \quad (2)$$

where T_0 — temperature of the aqueous electrolyte solution; ΔT — temperature change of the aqueous electrolyte solution; W — energy of metal ions.

The energy of discharging metal ions is determined by the following expression [10, 11]:

$$W = -\alpha z F(E - E_0, \quad (3)$$

where E — the current potential value; E_0 — the equilibrium potential value (E_0 = −0,96 V relative to the silver chloride electrode).

Table presents the energy values of the discharging zinc ions calculated by formula (3).

Based on the data on the stationary radial temperature distribution in the laser irradiation zone (Fig. 5, curve 1), we can calculate the radial distribution of zinc electrodeposition current density:

$$J(r) = J_0 \cdot \exp\{\frac{E_a \cdot \Delta t(r)}{R T_0 [T_0 + \Delta t(r)]}\}, \quad (4)$$

where J_0 = 1 A/m^2 — current density of zinc electrodeposition at T_0 = 296 K; $\Delta t(r)$ — temperature counted from T_0; E_a = 39 kJ/mol — activation energy of zinc electrodeposition; R — universal gas constant.

The values of current density calculated by expression (4), taking into account the data on the temperature in the laser irradiation zone (Fig. 5, curve 1) and the value of the metal ion discharge energy (Table), are close to the values of current density for the laser-enhanced process in the central part of

the laser irradiation zone. However, at $r > r_0$ (where r is a radial variable, r_0 is a laser beam radius) the temperature decreases, so the following modification of the equation is proposed to describe the radial dependence of the current density of laser-enhanced electrodeposition:

$$J(r) \cong j_0[1 - X(r - r_0)\frac{r - r_0}{r^* - r_0}] \cdot \exp[\frac{W \cdot \Delta T(r)}{RT_0[T_0 + \Delta T(r)]}], \quad (5)$$

where $X(r - r_0) = \begin{cases} 0, r \le 0 \\ 1, r > r_0 \end{cases}$ and r^* — stationary radius of the local coating of the deposited metal.

The application of expression (5) at temperatures corresponding to the course of the curve (Fig. 5, curve 1) and the value of the metal ion discharge energy (Table) gives a radial profile of the current density (Fig. 5, curve 2), from which we can see a decrease in the current density from the centre to the edge of the laser irradiation zone.

In connection with the practical application of laser-enhanced electrodeposition in the technology of protective coatings [12—17], it is important to find out the radial profile of the local coating thickness of zinc films under

Energy of the discharging zinc ions

Deposition modes	T, K	ω, W/m^2	W, kJ/mol (eV/ion)
DC	356	—	20,2 (0,21)
laser-enhanced electrodeposition		$70 \cdot 10^7$	38,5 (0,40)

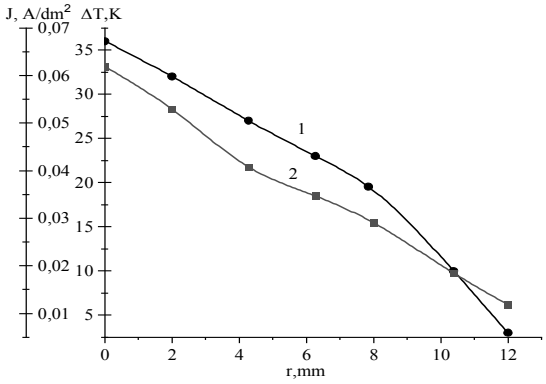

Fig. 5. Radial temperature (1) and current density (2) distribution in the laser irradiation zone (λ = 694 nm, ω = $70 \cdot 10^7$ W/m^2).

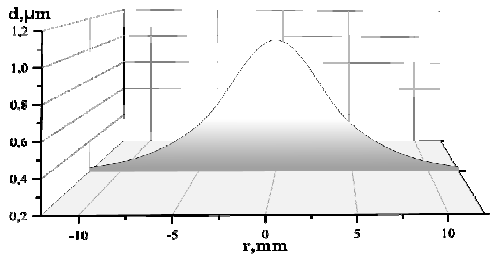

Fig. 6. Distribution of the coating thickness depending on the radial variable.

a *b*

Fig. 7. Local coatings in the form of: *a* — spot; *b* — lines (x20).

the selected optimum conditions. The local coating thickness d is proportional to the current density and electrodeposition time:

$$d(r) = \frac{k}{\rho} j(r)\tau = \frac{A}{\rho F} j(r)\tau, \tag{6}$$

where k — electrochemical equivalent (k_{Zn} = 0,34·10^{-6} kg/A·s); ρ — metal density (ρ_{Zn} = 7130 kg/m^3); A — atomic mass (A_{Zn} = 65,37·10^{-3} kg/mol); τ — time of the electrodeposition process; F — Faraday constant.

The results of the calculation of the local coating thickness as a function of the radial variable are shown in Fig. 6.

From the calculated data (Fig. 6) the thickness of the local coating decreases with increasing distance r from the centre ($r = r_0$) to the boundary of the focused laser beam and sharply decreases beyond it ($r > r_0$).

At local laser-enhanced electrodeposition of zinc, the average rate of zinc deposition in the area of the focused laser beam is 6,1 μm/h under optimal conditions of laser-enhanced electrodeposition (J = 4,6 A/m^2, E = −0,97 V), and the coating with a thickness of 0,08 μm, obtained at this potential at direct current, is deposited at laser-enhanced mode for a time τ ≈ 47 s.

In order to form a local metallic coating, the surface of which exceeds the diameter of the focused laser beam (Fig. 7, *a*), it is necessary to apply scanning, which was realised with translational movement of the cathode relative to the stationary laser beam (Fig. 7, *b*).

If υ is the linear velocity of uniform scanning, the formula for calculating the thickness of the local zinc line is as follows:

$$L(r,v) = \frac{\pi r_0 A_{Zn} N j(r,\upsilon)}{\rho \upsilon F z}, \tag{7}$$

where r_0 — radius of the focussed laser beam:; N — number of beam passes along the line route. At N = 30 and υ = 0,1 mm/s, the thickness of the local zinc coating is 0,05 μm, which corresponds to 188 atomic monolayers of zinc (zinc atom diameter d_{zn} = 0,266 nm).

At high values of radiation power, the temperature of the electrolyte solution in the near-cathode region significantly exceeds the temperature of the main volume of the electrolyte solution. As a result, the heated layers of the irradiation region are replaced by cooler nearby layers of the electrolyte solution and intensive mixing of the solution occurs. Convection flow leads to a decrease in the thickness of the diffusion layer at the cathode surface and to a reduction in the concentration of metal ions. Due to this, the film growth rate is significantly increased.

Conclusions

The optimal conditions for local laser electrodeposition of zinc on copper from sulfuric acid electrolyte were found, the parameters of local zinc spots and lines were calculated, and the speed of the electrodeposition process was estimated.

After technological elaboration the obtained results can be used in maskless processes of local galvanic deposition of zinc for repair of microdefects of protective coatings of the conductive elements of printed circuit boards.

References

1. Ren, Z., Hou, Y., Ba, Z., Wu, Y., Liu, M. (2025). Research progress on the fabrication of superhydrophobic surfaces via laser etching and electrodeposition hybrid techniques. Mater. Prot., Vol. 58, No. 5, pp. 12—31. https://doi.org/10.16577/j.issn.1001-1560.2025.0074
2. Bernasconi, R., Crimella, D., Gökhan Demir, A., Previtali, B., Magagnin, L. (2024). Laser assisted electrodeposition of binary metallic alloys from water-based electrolytes: The case of palladium-platinum. Surf. Coat. Technol., Vol. 484, pp. 130849. https://doi.org/10.1016/j.surfcoat.2024.130849
3. Song, J., Liao, Y., Liu, C., Lin, D., Qiao, L., Cheng, Y., Sugioka, K., Midorikawa, K., Zhang, S. (2012). Fabrication of gold microelectrodes on a glass substrate by femtosecond-laser-assisted electroless plating. J. Laser Micro Nanoeng., Vol. 7, pp. 334—338. https://doi.org/10.2961/jlmn.2012.03.0018
4. Zhou, R., Huang, T., Chen, L., Chen, S., Lin, S., Zhuo, Y. (2017). Electroless deposition of confined copper layers based on selective activation by pulsed laser iradiation. J. Laser Micro Nanoeng., Vol. 12, pp. 169—175. https://doi.org/10.2961/jlmn.2017.02.0021
5. Gupta, R. K, Singh, A., Singh, A., Ram Sankar, P., Sharma, S. K., Mukhopadhyay, P. K., Ganesh, P., Kaul, R., Bindra, K., Singh, B. (2018). Maskless copper electroplating on stainless steel using DPSS green laser. Surf. Eng., Vol. 34, pp. 446—453. https://doi.org/10.1080/02670844.2017.1396741
6. Yilin, Y., Jinqiu, Z., Peixia, Y., Maozhong, A. (2022). Laser-assisted electrodeposition technology and its application in the preparation of functional materials. Mater. Rep., Vol. 36, No. 3, pp. 20080209-9. https://doi.org/10.11896/cldb.20080209
7. Xueren, D., Kun, X., Zhaoyang, Z., Lingyue, Z., Yucheng, W., Hao, Z., Shuai, Y. (2021). Study on Cu—Al_2O_3 metal-matrix composite coating prepared by Laser-assisted electrodeposition. J. Electroanal. Chem., Vol. 904, No. 1, pp. 115855. https://doi.org/10.1016/j.jelechem.2021.115855
8. Kun, X., Wenrong, S., Shuai, Y., Yucheng, W., Douyan, Z., Zhihao, L., Yangfan, T., Hao, Z., Sishui, L., Zhaoyang, Z. (2023). Laser-enhanced electrodeposition preparation technology of superhydrophobic micro-nano structure coating. Colloids Surf. A Physicochem. Eng. Asp., Vol. 657, Part A, pp. 130507. https://doi.org/10.1016/j.colsurfa.2022.130507
9. Wenrong, S., Kun, X., Zhaoyang, Z., Sheng, G., Shuai, Y., Hao, Z., Sishui, L., Yucheng, W. (2022). Effect of laser on abnormal reduction process and properties evaluation of electrodeposited soft magnetic Fe—Ni coating. J. Electrochem. Soc., Vol. 169, No. 8, pp. 082507. https://iopscience.iop.org/article/10.1149/1945-7111/ac8646/meta
10. Tytarenko, V. V., Zabludovsky, V. O., Shtapenko, E. Ph., Tytarenko, I. V. (2022). Kinetic regularities of the formation of composite electrolytic coatings containing ultradispersed diamond particles. Phys. Chem. Solid St., Vol. 23, No. 3, pp. 461—467. https://doi.org/10.15330/pcss.23.3.461-467
11. Tytarenko, V. V., Zabludovsky, V. O., Tytarenko, I. V. (2024). Laser-assisted electrodeposition of composite carbon-containing nickel coatings. Nanosistemi, Nanomater., Nanotehnologii, Vol. 22, No. 1, pp. 41—52. https://doi.org/10.15407/nnn.22.01.041
12. Yucheng, W., Shuai, Y., Zhaoyang, Z., Kun, X., Weining, L., Wenrong, S., Hao, Z., Yang, L. (2022). Improvement of electrochemical deposition performance and design of Fe—Ni multilayer structure by nanosecond laser. Surf. Interfaces, Vol. 35, pp. 102458. https://doi.org/10.1016/j.surfin.2022.102458

13. Xu, M., Haiyun, Z., Yugang, Z., Xingang, H., Weisheng, L., Guangfen, J., Jianbing, M., Zengbo, Z., Jinjian, Z. (2023). Properties of Ni—Al_2O_3 composite coating by laser-assisted pulse electrodeposition. Appl. Opt., Vol. 62, No. 5, pp. 1384—1391. https://opg.optica.org/ao/abstract.cfm?URI=ao-62-5-1384
14. Wu, Y., Zhaoyang, Z., Zhihao, L., Jiabei, Z., Shuai, Y., Wenrong, S., Kun, X., Hao, Z., Yang, L. (2023). Improvement of the corrosion resistance of amorphous Ni—P coatings modified by a laser–electrodeposition hybrid process: Effect of morphology evolution on the electrochemical corrosion behavior. Appl. Surf. Sci., Vol. 624, pp. 157016. https://doi.org/10.1016/j.apsusc.2023.157016
15. Yucheng, W., Zhaoyang, Z., Kun, X., Jiabei, Z., Hao, Z., Yang, L., Shuai, Y., Wenrong, S. (2023). Electrochemical and immersion corrosion performance improvement of electrodeposited Fe—Ni coating: Effect of laser-induced periodic current on microstructure evolution. Corros. Sci., Vol. 219, pp. 111252. https://doi.org/10.1016/j.corsci.2023.111252
16. Yucheng, W., Zhaoyang, Z., Jiabei, Z., Shuai, Y., Kun, X., Hao, Z., Yang, L. (2024). Exploring the application of laser thermal effect in the multilayer gradient coatings designed by electrochemical deposition: Parameters, advancements, and limitations. J. Manuf. Process., Vol. 132, pp. 38—52. https://doi.org/10.1016/j.jmapro.2024.10.059
17. Zhen, Z., Guo, L., Tu, H., Zeying, W. (2025). A review of external field-enhanced metal electrodeposition: Mechanism and Applications. J. Miner. Met. Mater. Soc., Vol. 77, pp. 665—685. https://doi.org/10.1007/s11837-024-06968-7

Лазерно-стимульоване електроосадження локальних цинкових покриттів

В. В. Титаренко*, В. М. Горєв, А. М. Турінов, Т. Є. Воронк
Національний технічний університет “Дніпровська політехніка”
Україна, 49005, Дніпро, просп. Дмитра Яворницького, 19
*E-mail: tytarenko.valentina@gmail.com

https://orcid.org/0000-0001-6695-9810, https://orcid.org/0000-0002-9528-9497,
https://orcid.org/0000-0001-5815-6583, https://orcid.org/0000-0003-1781-8442

Представлено розроблений метод отримання локальних цинкових покриттів без масок за допомогою імпульсного лазера, промінь якого фокусується на катоді, розташованому в гальванічній ванні. Лазерне прискорення процесу осадження цинку зумовлене тепловим ефектом. Зондування зони термічного впливу мідно-константановою термопарою показало, що температура водного розчину електроліту у прикатодній області опромінювання лазерного променя радіусом 0,5 мм зростає від 293 до 356 К. Аналіз кривих катодної поляризації показав, що під час стимульованого електроосадження спостерігається збільшення густини струму та зсув потенціалу катода до позитивних значень порівняно з режимом осадження за допомогою постійного струму без лазерного опромінювання. Фіксується прискорення процесу електроосадження цинкових плівок у 9,4 рази при густині потужності лазера $70 \cdot 10^7$ Вт/м^2. Розраховано параметри локального цинкування та оцінено швидкість процесу електроосадження. Середня швидкість осадження цинку в області сфокусованого лазерного променя становить 6,1 мкм/год за оптимальних умов лазерно-стимульованого електроосадження (J = 4,6 А/м^2, E = -0,97 В), а покриття товщиною 0,08 мкм, отримане за цього потенціалу за допомогою постійного струму, осаджується при лазерно-стимульованому режимі протягом 47 с. Сканування поверхні катода лазерним випромінюванням призводить до формування локального металевого покриття, конфігурація якого відповідає траєкторії лазерного променя.

***Ключові слова**: електроосадження, лазерне випромінювання, катодна перенапруга, зона термічного впливу, локальне електролітичне покриття.*